SUPPLEMENTARY METHODS

Reagents

The amino acid sequence of the murine PS differs by about 20% compared to human PS. Our recent study[13] has demonstrated species specificity of PS bioactivities. Purified murine PS was a poor anticoagulant co-factor for murine activated protein C (APC) in human plasma. However, in mouse plasma, murine PS had good co-factor activity for murine APC. Human PS promoted more proliferation of human smooth muscle cells than for the mouse cells and similarly, cell proliferation potency of murine PS was higher for mouse cells than human cells. Accordingly, we used human PS in all studies with human BEC and murine PS in all studies with mouse models.

Primary human brain endothelial cells

In this, and in several earlier publications from our group,[32, S1-S7] primary human BEC were isolated from cortical tissue derived from patients who underwent brain surgery for epilepsy at the University of Rochester Medical Center. In the present study we used 5 different isolates. The age range of donors was between 14 and 52 years (4 females and 1 male). None of donors had vascular risk factors or any other concomitant disease except epilepsy. Epilepsy is associated with pathological changes in the hippocampus. Cortical tissue that was used for cell isolation was normal with no pathological changes. All BEC isolates were similarly characterized and displayed similar features. There were no differences in the purity between different samples. The BEC cells were > 99% pure, as measured by staining for the Von Willbrand Factor (endothelial cells) and negative immunostaining for the glial fibrillar acidic protein (astrocytes), CD11B (macrophage/microglia) and smooth muscle cell α-actin (SMA).

Primary human brain astrocytes

Primary cultures of human brain astrocytes were established using a previously described modified procedure.[S8,S9] Briefly, cortical tissue was obtained from patients subjected to brain surgery for epilepsy at the University of Rochester Medical Center, as described above. Tissue was minced, digested with 0.25% trypsin for 30 min at 37°C, and fractionated on a 30% Percoll gradient. The viable cell layer formed a wide, diffuse band between an upper layer containing myelin debris and a lower layer containing erythrocytes. The viable cell layer was carefully transferred to 50 mL centrifuge tubes and washed twice with PBS. Astrocytes were cultured in DMEM (with 1 g/L glucose, 5.9 g/L Hepes and 0.58 g/L glutamine; pH 7.4) containing 10% fetal bovine serum, G5 supplement (0.2 x, Invitrogen), 100 units/mL penicillin, and 100 mg/mL streptomycin. All astrocyte isolates were similarly characterized and displayed similar features. The astrocytes were > 99% pure as indicated by the GFAP staining, and were negative for macrophage/microglia (CD11b), endothelium (Von Willbrand Factor) or SMA (vascular smooth muscle cells).

In vitro model of the BBB

A single monolayer of human BEC was produced by placing 2×10^5 cells/cm^2 in the upper chamber of a 12-well tissue culture insert. Cells were cultured in Endogrow media for 3 days. At day 4, medium was replaced by RPMI 1640 supplemented with 0.1% FBS.

Oxygen/glucose deprivation (OGD) injury

Cell death was not observed in fully confluent human BEC BBB monolayers over 2 h OGD (a time period used for permeability, TER and molecular studies), as determined by the exclusion of trypan blue and release of LDH in the medium. In a limited number of permeability and TER measurements (Supplementary Fig. 1), OGD was extended to 24 h. Even at 24 h, there was < 5% cell death in the confluent endothelial monolayers subjected to OGD. In contrast, the subconfluent BEC cultures (60-80% confluency) are typically highly vulnerable to 24 h OGD challenge, as we reported.[32]

Analysis of the endothelial barrier by confocal microscopy

We performed triple immunostaining analysis for the zonula occludens (ZO-1) tight junction protein, F-actin and nuclei. The BBB monolayers were fixed for 30 min in 4% PFA and treated for 5 min with 0.2% Tween 20. We used a mouse polyclonal anti-human ZO-1 antibody (1:50, BD Biosciences, San Jose, CA) and an Alexa Fluor 488-conjugated donkey anti-mouse IgG (1:800, Invitrogen) as a secondary antibody. F-actin was stained with Alexa Fluor 568-conjugated phalloidin (1:50, Invitrogen). Nuclei were stained with Hoechst 33342 (1:10,000, Invitrogen). Tyro3 distribution in the basolateral and apical membranes of a monolayer was studied with a mouse monoclonal anti-human Tyro3 antibody (1:200, R&D sytems, Minneapolis, MN) followed by a secondary Alexa Fluor 488-conjugated donkey anti-mouse IgG (1:800, Invitrogen). We used a 543 nm HeNe laser to excite Alexa Fluor 568 and the emission was collected through a 560-615 bp filter, a 488 nm argon laser to excite Alexa Fluor 488 and the emission was collected through a 500-550 bp filter, and an 800 nm tuned Ti:sapphire laser (Mai Tai Spectra Physics) was used to excite Hoechst 33342 and the emission was collected through a 435-485 bp filter. Images were scanned using a Zeiss 510 meta confocal microscope with a Zeiss C-Apochromat 63×/1.2 NA water immersion objective (Carl Zeiss Microimaging Inc., Thornwood, NY).

Transmonolayer electrical resistance (TER)

TER values in control monolayers were in average ~ 270 Ω·cm^2 that is at the higher end of TER values determined in different *in vitro* BBB models from human, bovine and/or rodent brain endothelial cells.

The resistance of collagen-coated inserts was subtracted from the resistance obtained in the presence of the endothelial cultures. Human PS (5 to 100 nM) was added to the lower chamber. The TER control values in the present BBB monolayer model with primary human BEC were ~ 270 Ω·cm^2 that was somewhat higher that TER values typically determined in different *in vitro* BBB models using human, bovine and/or rodent brain endothelial monolayers in Transwells, as reported by different groups. For example, TER values between 30 and 80 Ω·cm^2 were reported for BBB monolayers using human BEC line HCMEC/D3[S10,S11] and ~ 200 Ω·cm^2 in a BBB

monolayer model using primary human BEC[S12]. A range of TER values was reported for BBB monolayers using primary bovine BEC from 123 Ω·cm[S11] at a higher end to lower values of 40 to 80 Ω·cm^2. [S12,S13] TER values between 168 and 18 Ω·cm^2 were reported for primary rat BEC BBB monlayers,[S15] and less than 30 Ω·cm^2 for rat BEC lines RBE4[S16] and GPNT[S17]. For the supplementary reference list see below in this section.

Permeability of the endothelial barrier

Briefly, the medium in upper chamber (apical side) of an established BBB monolayer was replaced with 500 µL FITC-labeled dextran solution (2 mg/mL) in phenol-red free DMEM. The lower chamber (basolateral side) containing 1,500 µL phenol-red free DMEM was sampled (20 µL) at 5 min intervals for 30 min. At each time point, 20 µL samples were taken from the upper chamber as well. The fluorescence intensity of each sample was determined using a fluorescence multiwell plate reader (Perkin Elmer Victor 3) at excitation/emission wavelength of 490/525 nm. The corresponding FITC-labeled dextran concentrations were determined from the standard curve.

Non-specific leakage of the human endothelial monolayer

Dextran (MW = 40,000 Da) used in this study was smaller than PS (MW ~ 69,000 Da). There is a non-specific diffusion of solutes in *in vitro* BBB systems allowing for some modest degree of free exchanges between the apical and basolateral side, as we reported[28]. In the present study, the percentage of dextran crossing the BBB under basal conditions (no OGD) from the basolateral to apical side at 1 h and 2 hs was 4.3% and 7.2%, respectively. And, from the apical to basolateral side 4.8% (1 h) and 7.7% (2 hs). Based on a theory of free diffusion of solutes across the pores of semi-permeable membranes, a non-specific diffusion of PS would be 0.76 of that for dextran, given the diffusion rates are inversely related to the reciprocal values of the square routes of their respective molecular weights.[27]

Silencing through RNA interference

Small interfering RNA (siRNA) targeting human Tyro3, Axl and $S1P_1$ were purchased from Santa Cruz Biotechnology. The corresponding scrambled siRNAs were used as controls. siRNAs targeting Tyro3, Axl and $S1P_1$ mRNA sequences and control siRNAs were transfected to primary human BEC using Santa Cruz Biotechnology transfection reagents and protocol. Cells were transfected 48 h before OGD treatment. Western blotting was used to verify inhibition of Tyro3, Axl and $S1P_1$ expression. PS was used at 100 nM.

Western blotting for Tyro3, Axl and Mer

Twenty µg of human brain endothelial lysates were analyzed by 4-15% Tris-HCL gel and transferred to nitrocellulose membranes (0.45 µm, Bio-Rad Laboratories, Hercules, CA). Membranes were blocked by 5% non-fat milk in TBS for 1 h and incubated overnight at 4°C with different primary antibodies. Primary mouse monoclonal anti-human Tyro3 antibody, goat monoclonal anti-human Axl antibody or mouse monoclonal anti-human Mer antibody (1:1000), from R&D systems (Minneapolis, MN) were used. Membranes were washed and incubated with

the corresponding secondary HRP-conjugated antibodies for 1 h. Immunoreactivity was detected using the SuperSignal® West Pico chemiluminescent substrate (Thermo Scientific, Rockford, IL).

Antibody blockade of TAM receptors

The antibodies used to block the TAM receptors were raised against the extracellular N-terminus domains of the respective TAM receptor family members. Axl blocking antibody was goat anti-human polyclonal raised against amino acids 33-440 (ligand binding site around 210) of the extracellular domain of human Axl. Tyro3 antibody was mouse monoclonal raised against amino acids 41-420 (ligand binding site around 210) of the extracellular domain of human Tyro3. Mer antibody was mouse monoclonal raised against amino acids 26-499 (ligand binding site around 100) against the extracellular domain of human Mer. The ligand binding sites for PS and Gas6 on the TAM receptors are located within the second immunoglobulin-like domain in their respective N-terminus extracellular domains[23].

Antibodies were added to the lower chamber at 10 μg/mL 60 min before PS (100 nM).

Rac1 activation assay

Briefly, human BBB monolayers were treated with 100 nM human PS. The cells were washed using ice cold PBS and lysed with a lysis buffer supplied in the kit. Cell lysates were centrifuged at 12,000 x g at 4°C for 5 min and supernatants incubated with PAK (p21 activated kinase 1 protein)-PBD [Rac/Cdc42 (p21) binding domain] beads at 4°C for 2 h. The beads were washed three times. Rac bound to beads was extracted by boiling each sample in Laemmli sample buffer. Samples from beads and total cell lysates were electrophoresed on 15% SDS-PAGE gels, transferred to nitrocellulose, blocked with 5% nonfat milk and analyzed by Western blotting using a monoclonal anti-Rac1 antibody (supplied with the kit). In addition, cell lysates from samples were immunoblotted with anti-Rac antibody as a protein loading control in each lane.

$S1P_1$ threonine phosphorylation

Human BBB monolayers were pretreated with vehicle, LY294002 (10 μM), control IgG (20 μg/ml) and anti-Tyro3 antibody (20 μg/ml; R&D Systems, Minneapolis, MN) for 60 min followed by either vehicle or PS (100 nM) treatment under OGD conditions for 10, 30 or 60 min. Cells were lysed using RIPA buffer. Samples were immunoprecipitated using a Protein G immunoprecipitation kit (Roche Applied Sciences, Indianapolis, IN) with a rabbit polyclonal anti-human $S1P_1$ antibody (Abcam, Cambridge, MA) followed by SDS-PAGE separation and transfer onto nitrocellulose membranes (Millipore Corp) and incubation with either anti-$S1P_1$ antibody (Abcam, Cambridge, MA) or anti-phosphothreonine antibody (Cell Signaling, Danvers, MA). Following incubation with the corresponding secondary HRP-conjugated antibodies, the immunoreactive products were detected with a chemiluminescent kit (Pierce, Rockford, IL).

Akt serine phosphorylation

Human BBB monolayers were pretreated with control IgG (20 μg/mL) or anti-Tyro3 antibody (20 μg/mL; R&D Systems, Minneapolis, MN) for 60 min followed by either vehicle or PS (100 nM) treatment under OGD conditions for 10, 30 or 60 minutes. Cells were lysed using RIPA buffer. Proteins (20 μg) were analyzed by 4-15% Tris-HCL gel and transferred to nitrocellulose membranes (0.45 μm, Bio-Rad Laboratories, Hercules, CA). The membranes were incubated overnight with primary rabbit polyclonal anti-mouse Phospho-Akt (Ser473) antibody or rabbit polyclonal anti-mouse Akt antibody diluted in 5% non-fat milk or 5% BSA in TBS, and then incubated with the corresponding secondary HRP-conjugated antibodies for 1 h. Immunoreactivity was detected using the ECL detection system (Amersham, Piscataway, NJ). The phopho-Akt signal was normalized to the total-Akt signal. Control pAkt levels under normoxic conditions were arbitrarily set as 1, and changes in pAkt levels under different conditions were expressed as a fold change compared to 1.

Isolation of mouse brain endothelial cells

Briefly, mouse brain cortices were dissected and rinsed with sterile PBS. Meninges and big vessels were removed carefully. The specimens were then homogenized in RPMI containing 2% FBS using a Dounce homogenizer. A 15% dextran solution was added to homogenates for separation of microvessels by dextran density gradient centrifugation. The pellet containing microvessels was resuspended in PBS/2% FBS and passed through 100 nm and 40 nm nylon filters in tandem to remove larger blood vessels and cell debris. The isolated microvessels were then digested in a solution containing 1 mg/ml collagenase/dispase in RPMI for 1 h at 37^{o}C. The digested microvessels were plated on rat-tail collagen-coated dishes and cultured in the endothelial growth media (MCDB131, 10% bovine plasma derived platelet-poor serum, endothelial cell growth supplement 60 μg/mL, heparin 15 U/mL, insulin 5 μg/mL, transferrin 5 μg/mL, selenium 5 ng/mL, penicillin/streptomycin 100 U/mL). Early passage 2-3 cells were used for experiments.

Because the objective of our study with mouse BEC was to determine which of the TAM receptors is involved in PS interaction, we felt that using a confluent model of mouse endothelial BBB with the tight junctions as in a human study would not be an absolute requirement to address this question. Therefore, we used a subconfluent cell cultures and an OGD model as we reported previously.[32]

PS quantification in CSF

In a separate group of control mice, CSF samples were collected from the cisterna magna 1 h after intravenous PS administration (0.2 mg/kg). Mice were anesthetized intraperitoneally with ketamine (100 mg/kg) and xylazine (10 mg/kg). The arachnoid membrane covering the cisterna magna was punctured using a 30G1/2 needle. The CSF was collected quickly using a narrow bore 20 μl micropipette tip (Rainin Instruments, LLC, Woburn, MA) and stored at -80°C until use. The CSF levels were determined by a quantitative Immunoblot analysis as we described.[13]

We used a quantitative Immunoblotting method as reported[13] to determine PS levels in mouse CSF. Briefly, recombinant mouse PS (3.75, 7.5, 15, 30, 45 ng) was used to generate standard curves. PS standards and CSF samples (10-30 μL) were subjected to 4-12% NuPAGE® Bis-Tris SDS-PAGE (Invitrogen) and transferred to nitrocellulose membranes (BioRad). Membranes

were blocked with 5% non-fat milk in TBST (10 mM Tris pH 7.5, 150 mM sodium chloride, 0.05% Tween 20) for 1 h and incubated overnight with either anti-mouse PS (A0384, DakoCytomation) or anti-human PS (AF4036, R&D systems, Minneapolis, MN) in TBST. The membranes were then washed and incubated with an HRP-conjugated secondary antibody for 1 h. Immunoreactivity was detected using SuperSignal® West Pico chemiluminescent substrate (Thermo Scientific). PS band intensity was determined by densitometric scanning (AlphaImager™ 2200, Alpha Innotech Corp., San Leandro, CA). PS concentrations in CSF (nM/L) were calculated from standard curves. PS signal from CSF samples was within a linear range of PS standards.

Transient middle cerebral artery occlusion (MCAO)

Motor neurological score was determined on a scale 0 to 5: no neurological deficit (0), failure to extend left forepaw fully (1), turning to left (2), circling to left (3), inability to walk spontaneously (4) and stroke-related death (5).

The infarction volume was obtained by subtracting the edema volume from the injury volume. Edema volume (tissue swelling) was calculated by subtracting the volume of the contralateral nonischemic hemisphere from the volume of the ipsilateral ischemic hemisphere as we described.[S19]

To the best of our knowledge the BBB transport of W146 has not been measured. However, it has been reported that ^{14}C-labeled FTY720 (MW = 343), an analog of W146, crosses easily the BBB.[S18] W146 (MW = 342) has the same number of H-bond donors as FTY720, but has 2 more H-bond acceptors (i.e., 5 vs. 3) that might result in somewhat lower permeability across the BBB compared to FTY720. Nevertheless, our data showing that W146 given 10 min before the MCAO can block the effect of PS confirms in an experimental model that W146 can cross the BBB in a sufficient amount to reach the basolateral side where Tyro3 is predominantly localized *in vivo* and block the activation of $S1P_1$ (Fig. 5H).

Tyro3 localization (abluminal vs. luminal) in brain endothelium *in situ*

Paraffin-embedded 7 µm thick coronal sections from 3 month-old C57BL/6 mouse cortex were deparaffinized with xylene and rehydrated with serial ethanol washes. Slides were then boiled in antigen unmasking solution (Vector Laboratories; H-3300) as described by the manufacturer. Sections were rinsed with PBS and blocked for 1 h in PBS containing 5% normal swine serum, 0.05% triton X-100, and 0.1% bovine serum albumin. Slides were incubated overnight at 4º C with goat polyclonal anti-aquaporin 4 1:50 (Santa Cruz Biotechnology; sc-9888) and rabbit polyclonal anti-Tyro3 1:25 (Abcam; ab37841). Dylight 549-conjugated bovine anti-goat IgG (Jackson Laboratories; 805505180) and biotin-conjugated donkey anti-rabbit IgG (Jackson Laboratories; 711065152) followed by AMCA-conjugated streptavidin were used to detect Aquaporin-4 and Tyro3, respectively. Fluoroscein-conjugated Lycopersicon Esculentum Lectin (Vector Laboratories; FL-1171) was diluted 1:500 and then applied to the sections for 75 min at 37º C to detect endothelial cells. Sections were scanned using a Zeiss 510 meta confocal microscope with a C-Apochromat 40×/1.2 NA water immersion objective (Carl Zeiss Microimaging Inc.). A 488 nm argon laser was used to excite fluoroscein and the emission was collected through a 500-550 bp filter, and a 543 HeNe laser was used to detect Dylight 549 as

described above. Images and signal intensity at the luminal and abluminal sides were acquired by comparing the distribution of Tyro3 signal intensity in an overlapping lectin-positive endothelial area by using the Zeiss Zen 2008 software (Carl Zeiss Microimaging Inc.). Astrocyte-specific aquaporin 4 staining served to confirm position of the brain-facing abluminal side of endothelium. The vessel lumen was used to confirm position of the blood-facing luminal side of endothelium.

Tyro3, Axl and Mer in mouse brain microvessels

Ten μg of brain microvascular lysate proteins were subjected to 4-12% NuPAGE® Bis-Tris SDS-PAGE (Invitrogen) and transferred to nitrocellulose membranes (BioRad). Membranes were blocked with 5% non-fat milk in TBST for 1 hr and incubated overnight with the following primary antibodies: Tyro3 (AF759, R&D), Axl (AF854, R&D) and Mer (AF591, R&D). The membranes were washed and incubated with horseradish peroxidase-conjugated secondary antibody for 1 h. Immunoreactivity was detected using SuperSignal® West Pico chemiluminescent substrate (Thermo Scientific).

Supplementary Methods References

S1. Guo H, Singh I, Wang Y, et al. Neuroprotective activities of activated protein C mutant with reduced anticoagulant activity. *Eur J Neurosci.* 2009;29(6):1119-1130.

S2. Guo H, Wang Y, Singh I, et al. Species-dependent neuroprotection by activated protein C mutants with reduced anticoagulant activity. *J Neurochem.* 2009;109(1):116-124.

S3. Deane R, LaRue B, Sagare AP, et al. Endothelial protein C receptor-assisted transport of activated protein C across the mouse blood-brain barrier. *J Cereb Blood Flow Metab.* 2009;29(1):25-33.

S4. Thiyagarajan M, Cheng T, Zlokovic BV. Endothelial cell protein C receptor: role beyond endothelium? *Circ Res.* 2007;100(2):155-157.

S5. Cheng T, Petraglia AL, Li Z, et al. Activated protein C inhibits tissue plasminogen activator-induced brain hemorrhage. *Nat Med.* 2006;12(11):1278-1285.

S6. Domotor E, Benzakour O, Griffin JH, et al. Activated protein C alters cytosolic calcium flux in human brain endothelium via binding to endothelial protein C receptor and activation of protease activated receptor-1. *Blood.* 2003;101(12):4797-4801.

S7. Cheng T, Liu D, Griffin JH, et al. Activated protein C blocks p53-mediated apoptosis in ischemic human brain endothelium and is neuroprotective. *Nat Med.* 2003;9(3):338-342.

S8. Lue LF, Brachova L, Walker DG, et al. Characterization of glial cultures from rapid autopsies of Alzheimer's and control patients. *Neurobiol Aging.* 1996;17(3):421-429.

S9. De Groot CJA, Langeveld CH, Jongenelen CAM, et al. Establishment of human adult astrocyte cultures derived from postmortem multiple sclerosis and control brain and spinal cord regions: Immunophenotypical and functional characterization. *J Neurosci Res*. 1997;49(3):342-354.

S10. Cucullo L, Couraud PO, Weksler B, et al. Immortalized human brain endothelial cells and flow-based vascular modeling: a marriage of convenience for rational neurovascular studies. *J Cereb Blood Flow Metab*. 2008;28(2):312-328.

S11. Weksler BB, Subileau EA, Perriere N, et al. Blood-brain barrier-specific properties of a human adult brain endothelial cell line. *FASEB J*. 2005;19(13):1872-1874.

S12. Zenker D, Begley D, Bratzke H, et al. Human blood-derived macrophages enhance barrier function of cultured primary bovine and human brain capillary endothelial cells. *J Physiol*. 2003;551(3):1023-1032.

S13. Inglis VI, Jones MP, Tse AD, et al. Neutrophils both reduce and increase permeability in a cell culture model of the blood-brain barrier. *Brain Res*. 2004;998(2):218-229.

S14. Mark KS, Davis TP. Cerebral microvascular changes in permeability and tight junctions induced by hypoxia-reoxygenation. *Am J Physiol Heart Circ Physiol*. 2002;282(4):H1485-1494.

S15. Calabria AR, Weidenfeller C, Jones AR, et al. Puromycin-purified rat brain microvascular endothelial cell cultures exhibit improved barrier properties in response to glucocorticoid induction. *J Neurochem*. 2006;97(4):922-933.

S16. Rist RJ, Romero IA, Chan MWK, et al. F-actin cytoskeleton and sucrose permeability of immortalised rat brain microvascular endothelial cell monolayers: effects of cyclic AMP and astrocytic factors. *Brain Res*. 1997;768(1-2):10-18.

S17. Romero IA, Radewicz K, Jubin E, et al. Changes in cytoskeletal and tight junctional proteins correlate with decreased permeability induced by dexamethasone in cultured rat brain endothelial cells. *Neurosci Lett*. 2003;344(2):112-116.

S18. Foster CA, Howard LM, Schweitzer A, et al. Brain penetration of the oral immunomodulatory drug FTY720 and its phosphorylation in the central nervous system during experimental autoimmune encephalomyelitis: Consequences for mode of action in multiple sclerosis. *J Pharmacol Exp Ther*. 2007;323(2):469-476.

S19. Wang Y, Thiyagarajan M, Chow N, et al. Differential neuroprotection and risk for bleeding from activated protein C with varying degrees of anticoagulant activity. *Stroke*. 2009;40(5):1864-1869.

Supplementary Table 1: Physiological parameters before MCAO, during MCAO and 60 min after MCAO. Hct – Hematocrit, MBP – mean arterial blood pressure, VH – Vehicle, PS – protein S. No significant difference was observed between any of the groups. (Mean ± SEM, $n = 3$)

	PaO_2 (mm Hg)			PCO_2 (mm Hg)			pH			Hct (%)			MBP (mm Hg)		
	Pre MCAO	MCAO	Post MCAO	Pre MCAO	MCAO	Post MCAO	Pre MCAO	MCAO	Post MCAO	Pre MCAO	MCAO	Post MCAO	Pre MCAO	MCAO	Post MCAO
Tyro3$^{+/+}$ + VH	79.5±6.2	76.8±4.9	75.2±5.3	45.5±4.3	47.8±2.7	44.9±3.6	7.24±0.03	7.22±0.04	7.21±0.02	39.2±3.5	42.5±4.1	40.4±3.3	72.3±3.8	75.4±3.2	71.3±4.3
Tyro3$^{+/+}$ + PS	81.2±5.4	75.3±6.2	77.2±3.8	42.6±1.9	45.3±2.2	48.2±1.6	7.32±0.02	7.28±0.04	7.25±0.05	38.2±2.9	39.4±2.5	35.8±3.4	78.3±2.9	72.6±5.3	77.2±4.4
Tyro3$^{-/-}$ + VH	75.4±3.1	70.6±5.2	74.3±4.7	43.8±2.9	44.2±3.1	47.2±3.8	7.26±0.02	7.24±0.04	7.21±0.04	44.2±2.5	41.3±3.5	43.9±4.2	78.2±4.9	76.3±5.9	74.2±5.8
Tyro3$^{-/-}$ + PS	78.2±4.3	80.2±5.3	81.5±7.4	41.9±1.8	45.3±2.3	48.2±3.6	7.32±0.05	7.28±0.02	7.23±0.02	38.8±2.7	36.6±2.9	34.2±2.6	73.5±6.2	76.2±4.8	79.3±7.3
Axl$^{-/-}$ + VH	80.5±2.6	74.5±3.6	77.6±2.8	45.2±3.7	43.5±1.9	46.7±4.2	7.35±0.03	7.26±0.05	7.26±0.02	40.5±2.8	42.2±4.1	45.3±4.9	69.8±5.2	72.2±5.7	76.4±5.6
Axl$^{-/-}$ + PS	82.2±7.4	80.5±4.4	78.5±5.2	42.9±2.3	45.3±1.8	46.5±4.7	7.34±0.02	7.28±0.06	7.21±0.03	41.2±3.3	43.4±2.5	38.8±3.2	72.5±4.8	77.4±6.4	75.2±3.8
Mer$^{-/-}$ + VH	78.8±6.6	80.2±4.2	76.4±8.2	47.2±3.3	45.8±4.5	46.3±3.5	7.31±0.04	7.28±0.04	7.22±0.05	38.3±2.9	35.5±3.2	36.5±3.7	76.7±3.9	74.2±3.8	76.3±4.9
Mer$^{-/-}$ + PS	80.5±4.7	81.1±6.3	79.5±4.6	43.5±3.7	44.6±4.2	41.3±3.8	7.33±0.06	7.22±0.03	7.24±0.05	36.5±2.5	34.2±3.4	38.4±2.9	73.5±4.4	72.4±5.8	76.8±6.4

Supplementary Figure Legends

Supplementary Figure 1. Protein S protects the endothelial barrier integrity from OGD within 24 h. A, Confocal scanning microscopy of a human brain endothelial monolayer 24 h after normoxia or OGD with and without PS. ZO1, green; F-actin, red; Nuclei, blue. Scale bar = 10 μm. B, Transmonolayer endothelial resistance (TER) 24 h after normoxia or OGD with or without PS. C, Permeability of BBB monolayers (P) to FITC-dextran 24 h after normoxia or OGD with or without PS. In all studies human PS was used at 100 nM. Mean ± SEM, from 3 to 6 independent cultures.

Supplementary Figure 2. No effect of OGD on Tyro3 phosphorylation or Tyro3-$S1P_1$ interaction. A, Tyro3 phosphorylation in human BBB monolayers under normoxia or OGD; IP, immunoprecipitation of phospho-tyrosine proteins; IB, immunoblotting of Tyro3. B, IP of $S1P_1$ with anti-Tyro3 (C-terminus) antibody in BBB monolayers under normoxia or OGD. IB, immunoblotting of $S1P_1$ and Tyro3. C, Inhibition of $S1P_1$ expression in endothelial monolayers after transfection with $S1P_1$ siRNA compared to control siRNA determined by immunoblotting.

Supplementary Figure 3. Low dose W146 does not affect the BBB permeability *in vivo*. A, Blood-brain barrier permeability to F-dextran (70 kDa) in sham-operated mice treated with vehicle without $S1P_1$-specific antagonist W146 treatment. B-C, W146 at a low dose (1 mg/kg) administered intraperitoneally does not alter the blood-brain barrier permeability to F-dextran (70 kDa) in sham-operated mice treated with vehicle (B) or murine protein S (0.2 mg/kg intravenously) (C) as shown by 2-photon microscopy. Scale bar = 20 μm.

Supplementary Figure 1

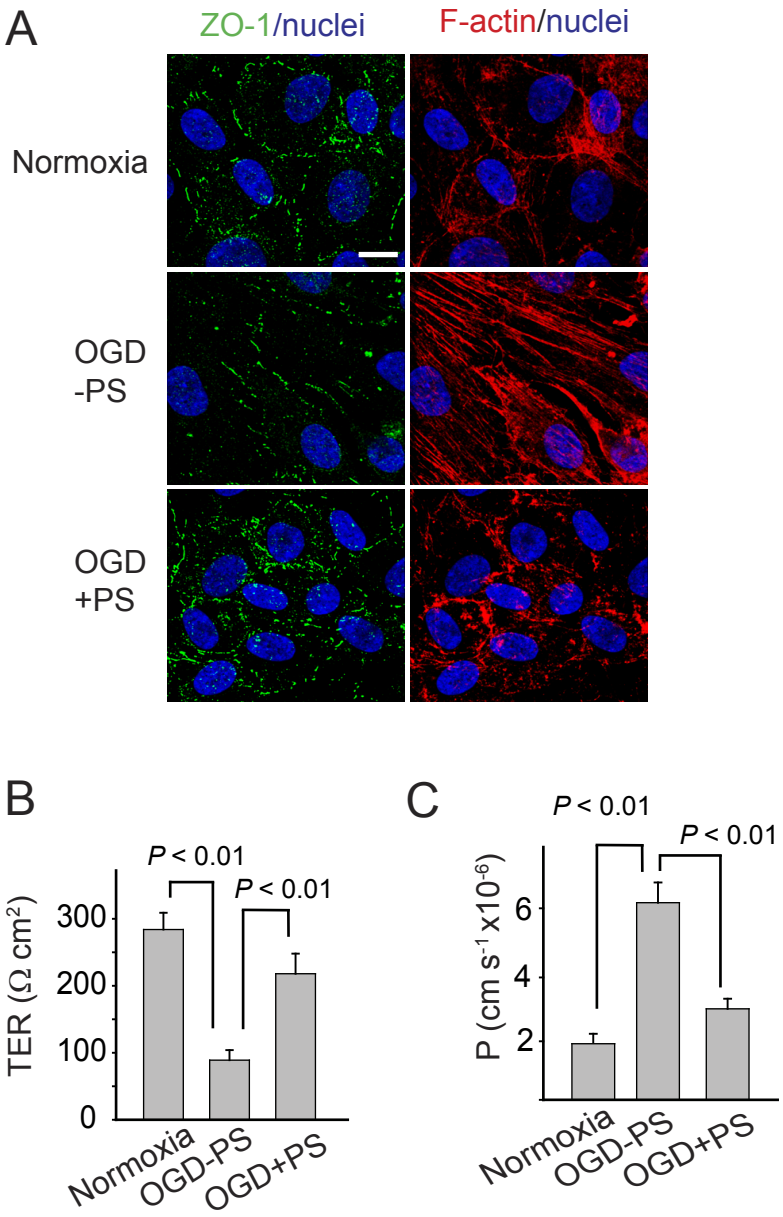

Supplementary Figure 2

A

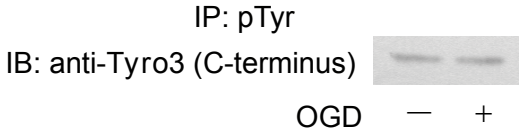

B

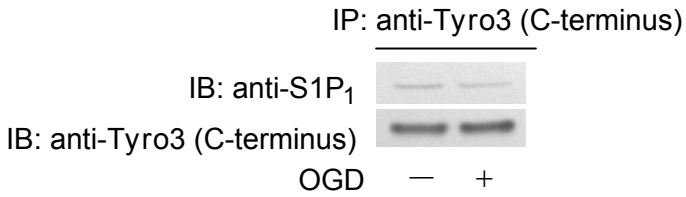

C

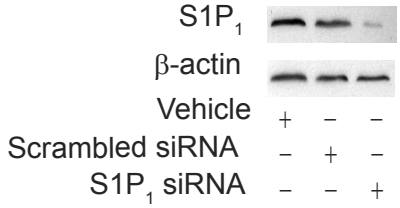

Supplementary Figure 3

Sham-operated *Tyro3*$^{+/+}$ - W146

Sham-operated *Tyro3*$^{+/+}$ + W146

A Vehicle

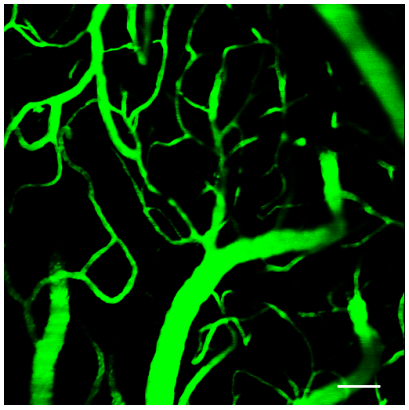

B Vehicle

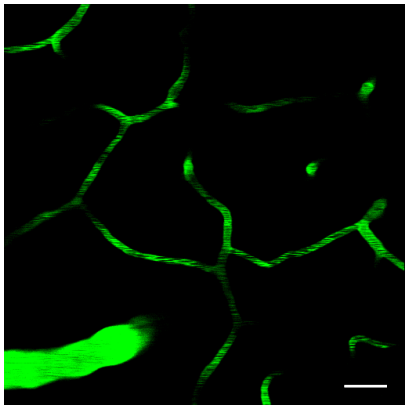

C PS